

# Topologically Controlled Intracavity Laser Modes Based on Pancharatnam-Berry Phase

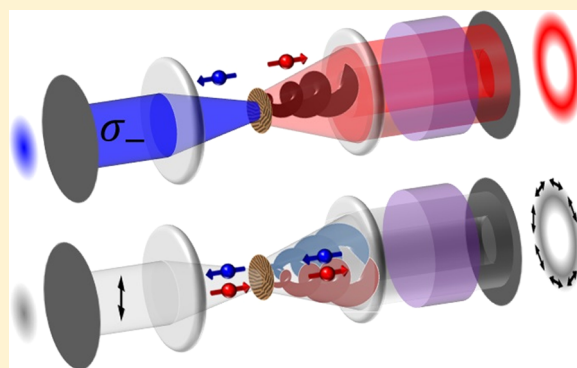
Elhanan Maguid,<sup>†,§</sup> Ronen Chriki,<sup>‡,§</sup> Michael Yannai,<sup>†</sup> Vladimir Kleiner,<sup>†</sup> Erez Hasman,<sup>†</sup> Asher A. Friesem,<sup>‡</sup> and Nir Davidson<sup>\*,‡</sup>

<sup>†</sup>Micro and Nanooptics Laboratory, Faculty of Mechanical Engineering and Russell Berrie Nanotechnology Institute, Technion – Israel Institute of Technology, Haifa 3200003, Israel

<sup>‡</sup>Weizmann Institute of Science, Department of Physics of Complex Systems, Rehovot 7610001, Israel

**ABSTRACT:** Incorporation of a metasurface that involves spin-orbit interaction phenomenon into a laser cavity provides a route to the generation of spin-controlled intracavity modes with different topologies. By utilizing the geometric phase, Pancharatnam-Berry phase, we found a spin-enabled self-consistent cavity solution of a Nd:YAG laser with a silicon-based metasurface. Using this solution we generated a laser mode possessing spin-controlled orbital-angular momentum. Moreover, an experimental demonstration of a vectorial vortex is achieved by the coherent superposition of modes with opposite spin and orbital angular momenta. We experimentally achieved a high mode purity of  $\sim 95\%$  due to laser mode competition and purification. The photonic spin-orbit interaction mechanism within a laser-cavity can be implemented with multifunctional shared-aperture nanoantenna arrays to achieve multiple intracavity topologies.

**KEYWORDS:** meta-surface, optical resonator/cavity, topology, laser beam shaping, nanophotonics, Berry phase



Manipulation of the lasing mode has been achieved in the past by inserting engineered optical elements inside a laser cavity to control the properties of the output beam.<sup>1–6</sup> Specific examples include (i) intracavity binary masks, amplitude, and phase masks, and diffractive elements for obtaining pure and high order laser modes,<sup>4,7,8</sup> (ii) intracavity polarization elements to obtain radial and azimuthal polarizations,<sup>9</sup> and (iii) intracavity optical elements to achieve efficient phase locking and beam combining.<sup>10,11</sup> Moreover, intracavity elements in degenerate or near degenerate cavity lasers enable to form large arrays of lasers<sup>12</sup> with tunable spatial coherence<sup>13,14</sup> and to focus light through a rapidly changing scattering medium.<sup>2</sup>

Incorporation of a metasurface element, which involves spin-orbit interaction phenomenon, into a laser-cavity may leverage the generation of exotic modes that can be controlled by coupling the spin and orbital angular momentum (OAM) of photons traveling inside the cavity.<sup>15–18</sup> A metasurface is an engineered array of subwavelength nanostructures which enhance light-matter interactions and modulate electromagnetic wave scattering properties.<sup>19–29</sup> By varying the local in-plane orientations  $\theta(x, y)$  of these nanostructures, a geometric phase mechanism is obtained,<sup>30,31</sup> forming Pancharatnam-Berry phase optical elements (PBOEs).<sup>15,19,20</sup> Specifically, the local in-plane orientations  $\theta(x, y)$  of the PBOE cause phase delays according to  $\phi_g(x, y) = -2\sigma\theta(x, y)$ , where  $\sigma = \sigma_{\pm} = \pm 1$  denotes the sign of spin angular momentum of light ( $\hbar\sigma_{\pm}$ ). The

polarization helicity of light is defined as right (left) circular polarization if the direction of its spin is the same as (opposite to) the direction of propagation.

Recently, reflective PBOEs were exploited as output couplers in a solid state laser to obtain scalar vortex beams carrying OAM and optical vectorial vortex beams.<sup>32</sup> As output couplers, the PBOEs do not interact with the laser cavity and do not affect the lasing mode. Also, single mode operation of THz quantum cascade lasers was achieved by focusing light with metasurfaces, and active metasurface waveguide arrays were used to control and switch between the two polarizations of a THz quantum cascade laser.<sup>33,34</sup>

Here, we report on the incorporation of a PBOE into a laser in order to achieve a topologically controlled intracavity mode, as shown schematically in Figure 1. This work is the first demonstration of intracavity mode control by the use of dielectric metasurface. Specifically, we designed an efficient dielectric PBOE based on silicon nanoantennas operating in transmission mode shown in Figure 2a. The nanoantennas were 100 nm wide and 400 nm deep, arranged 300 nm apart from each other (center to center) within a diameter of 200  $\mu\text{m}$ . Finite difference time domain simulation predicted a theoretical metasurface efficiency of 82% at a wavelength of 1.064  $\mu\text{m}$ , whereas the experimental efficiency was found to be 73%, due

Received: December 12, 2017

Published: March 15, 2018

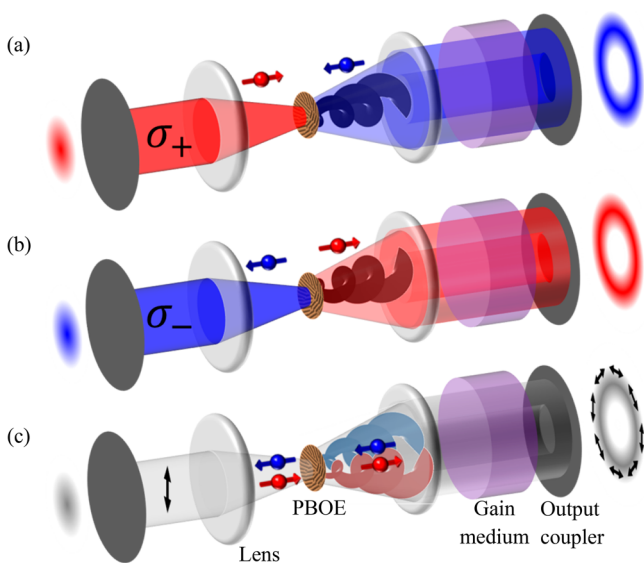


**Figure 1.** Topologically controlled intracavity laser mode. (a–c) Intracavity spin-controlled laser mode based on a PBOE that generates modes with topological charge of (a)  $l = 1$ , (b)  $l = -1$ , and (c) vectorial vortex. Red and blue helices denote scalar vortices of opposite spin and OAM. The self-consistent solution of the topologically controlled intracavity laser mode is a Gaussian emitted to the left and a higher topology beam to the right.

to fabrication imperfections. This efficiency results from the limited transmittance (experimentally  $\sim 77\%$ ) and internal conversion efficiency from spin-up to spin-down (experimentally  $\sim 95\%$ ). Thus, most of the reduction in efficiency is due to reflections. To control the topological charge of the mode, the nanoantennas were oriented according to  $2\theta = l\varphi$ , where  $l$  is the topological charge and  $\varphi$  is the azimuthal angle. The spin-enabled PBOE<sup>15</sup> can be described by an operator  $\hat{O}_{\text{PBM}}$ , where  $\hat{O}_{\text{PBM}}|\sigma_{\pm}\rangle = \exp(i\sigma_{\pm}l\varphi)|\sigma_{\pm}\rangle$ .

We experimentally investigated the intensity distribution after a single and double pass through the PBOE, using Nd:YAG laser light at a wavelength of  $1.064 \mu\text{m}$ , as shown in Figure 2b. After passing through the PBOE once, the incident Gaussian beam of spin-up state  $|\sigma_+\rangle$  is converted to a spiral phase beam with spin-down according to  $\hat{O}_{\text{PB}}|\sigma_+\rangle = e^{il\varphi}|\sigma_-\rangle$ . After reflection from a mirror, the direction of propagation is reversed, but the spin is not affected.<sup>35</sup> Consequently, the emerging beam is converted back to a Gaussian beam with

spin-state,  $\hat{O}_{\text{PB}}e^{il\varphi}|\sigma_-\rangle = |\sigma_+\rangle$ . Note, if the reflected beam does not pass back through the PBOE, it maintains the converted OAM state.

The PBOEs are therefore especially suitable for intracavity mode shaping, as they easily supply a self-consistent solution after every round trip (double pass) through the elements. For comparison, a double pass through a standard spiral phase element results in accumulation of twice the OAM. Therefore, a self-consistent solution with a spiral phase element would require two such elements, which would generate the OAM and then cancel it out. Indeed, several methods that were previously demonstrated for generating beams with OAM inside a laser cavity were prone to use two elements inside the laser cavity, which had to be carefully aligned.<sup>7</sup>

In order to demonstrate a topologically controlled intracavity laser mode, the PBOE was placed inside a modified degenerate cavity laser, as schematically shown in Figure 3a. The laser cavity was comprised of two flat mirrors, a gain medium, a circular aperture, and two lenses in a 4f telescope arrangement. The two mirrors of the cavity had 80% reflectivities, so the output power could be measured at either side of the cavity. The gain medium was 10 cm long and had a diameter of 4 mm, and it was pumped with a Xenon flash lamp in quasi-CW 100  $\mu\text{s}$  long pulses at 1 Hz repetition rate in order to avoid thermal lensing effects. The lenses had a focal length of 15 cm, and the diameter of the intracavity circular aperture was  $200 \mu\text{m}$ , chosen to match the size of the PBOE and ensure that all energy in the cavity propagates through it. The PBOE of  $200 \mu\text{m}$  diameter was placed at the Fourier plane between the two lenses adjacent to the circular aperture and near the gain medium. In order to enforce circular polarization of  $\sigma_+$  or  $\sigma_-$  upon the lasing mode, a quarter-wave plate, a Faraday rotator, and a linear polarizer were placed inside the cavity. The laser polarization could be switched between  $\sigma_+$  and  $\sigma_-$  by changing the orientation of the quarter-wave plate, and setting it at either  $+45^\circ$  or  $-45^\circ$  relative to the orientation of polarization of the incident beam. The circular aperture served as a spatial filter, introducing loss to high order modes and forcing the laser to operate with a single mode.

Figure 3a shows the experimental output intensity distributions from the two sides of the laser cavity. As expected, at one side the distribution has the shape of a doughnut, whereas at the other side it has the shape of a Gaussian. The OAMs of the doughnut shaped intensity profile were determined using a Mach–Zehnder interferometer. Specifically,

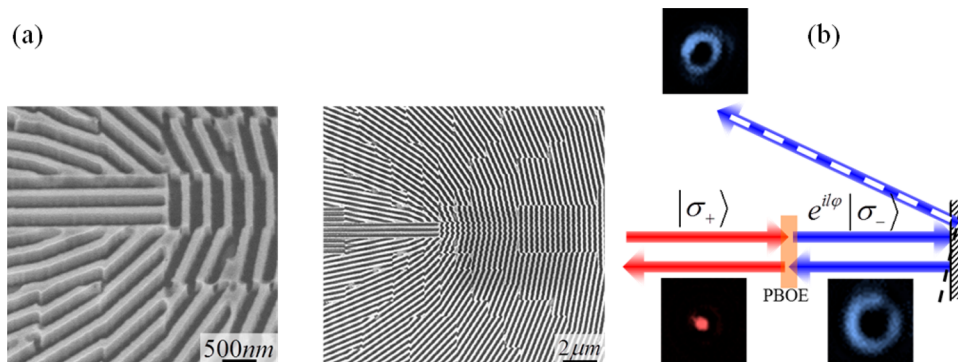


**Figure 2.** Spin-enabled self-consistent concept based on PBOE. (a) Side and top view of scanning electron microscope images of the fabricated silicon-based spiral PBOE. (b) Operation and experimental results for single and double passes through the metasurface outside the laser cavity for incident Gaussian beam (red). Red and blue denote spin-up and spin-down states, respectively.

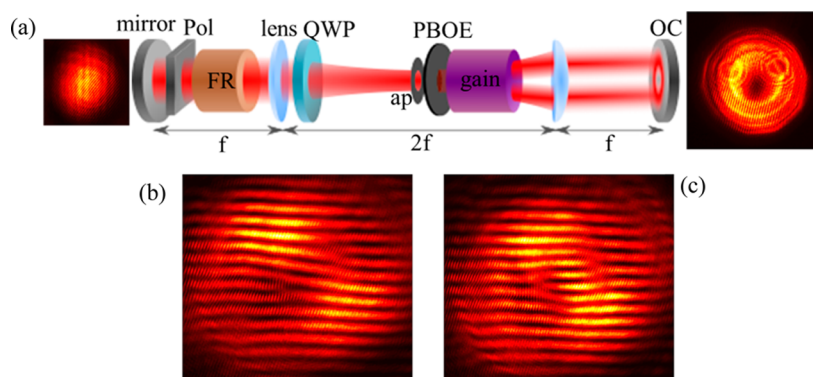


**Figure 3.** Spin-controlled OAM laser modes. (a) Spin-controlled modified degenerate laser cavity. Polarizer (Pol), Faraday rotator (FR), and quarter-wave plate (QWP) serve to control the polarization of the intracavity mode. Experimental results of the spin-dependent intracavity laser modes; OAM beam at left (mirror) and Gaussian beam at right (OC, output coupler). (b, c) Self-interference patterns of the OAM mode, indicating (b) OAM of  $l = +1$  for spin-up and (c) OAM of  $l = -1$  for spin-down.

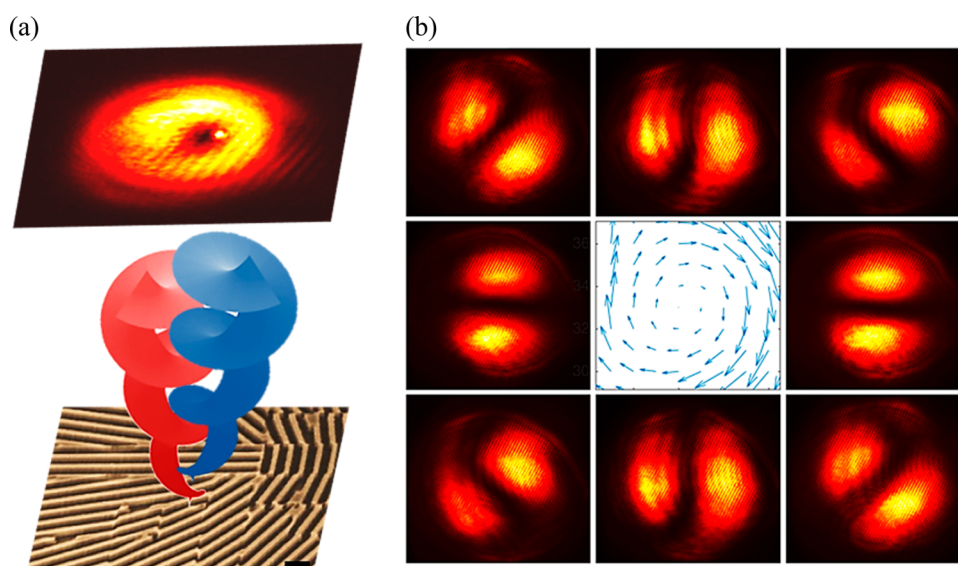


**Figure 4.** Intracavity vectorial vortex mode for a laser with azimuthally polarized output beam. (a) Schematic illustration of the intracavity vectorial vortex and the corresponding experimental intensity distribution. Red and blue helices denote opposite spin states, and the black scale-bar in the colored scanning electron microscope image is 500 nm. (b) Experimental intensity distributions obtained at eight different linear polarizer orientations and the resultant azimuthal polarization vector field, as obtained from measured Stokes parameters.

the output of the laser was split into two arms and a slight angle and shift was introduced in one of the arms, and then the light from the two arms were combined and detected as an interference pattern. The experimental interference patterns are shown in Figure 3b,c. As is evident, two shifted “forks” are clearly visible, indicating a spin-dependent topological charge of  $\pm 1$ , where the sign of the OAM is inferred by the relative orientation of the “forks”. The purity of the mode, defined as the normalized overlap integral between the detected and expected intensity distributions, was measured to be 95.7%.

In a cavity with no gain (“cold cavity”), there is no preference to having the vortex beam on one side of the cavity or on the other. There is perfect degeneracy between these two solutions, and consequently, a superposition of Gaussian and vortex beams are expected to lase on either side of the cavity. However, the presence of the gain breaks the degeneracy, and strongly prefers the solution where the vortex beam overlaps the gain, as was indeed measured experimentally (Figure 3a). Since the vortex beam has a larger mode area as compared to a Gaussian beam (by a factor of  $e \sim 2.71$ ), this solution has

substantially higher gain and is, therefore, the only lasing mode due to mode competition.

Moreover, placing the PBOE also improves its effective efficiency. To see this, notice that the basic mechanism of the cavity is based on the notion that any beam returns to its initial state after a double pass through the PBOE, as explained above. As a result, the noninteracting reflected light is identical in spin and OAM to the light that went through the element twice, and it therefore does not reduce the purity of the output beam. The reflected light is not lost, but rather is injected back into the cavity for further buildup of the lasing mode, thereby increasing the effective efficiency of the PBOE.

The PBOEs can also form vectorial vortices,<sup>19</sup> thereby increasing the realm of intracavity topological effects. For example, vectorial vortices with spiral PBOE can be obtained by tailoring the relative phase of two opposite spins according to  $\hat{O}_{PB}(|\sigma_+\rangle - |\sigma_-\rangle) = e^{-i\varphi}|\sigma_-\rangle - e^{i\varphi}|\sigma_+\rangle$ . When placing a PBOE inside a laser cavity of linearly polarized light, the emerging field consists of two opposite spin and OAM states. Experimentally, the quarter-wave plate and Faraday rotator were removed from

the cavity. The intracavity superposition of  $l = 1$  and  $l = -1$  resulted in a mode having azimuthal polarization, as shown in Figure 4a. The polarization state of the output beam was measured by projecting the vectorial vortex on a linear polarizer (Figure 4b). By measuring the Stokes parameters, we determined that the average deviation of the expected azimuthal angle is  $13^\circ$  and the average ellipticity angle  $16^\circ$ , indicating polarization purity of  $\sim 94\%$ .

The implementation of the spin-orbit interaction mechanism within a laser-cavity provided the route to control the topology of the lasing mode in a spin-dependent manner. As we showed, the intracavity PBOE interacted with the laser cavity and improved performances: the effective efficiency of the PBOE was improved and the output power was increased due to an enhanced mode area on the gain. The Pancharatnam-Berry phase is wavelength-independent,<sup>25,36</sup> so unlike other phase elements, the PBOEs are also suitable for tunable and ultrafast (femtoseconds) lasers. Moreover, the PBOEs are flat so they are CMOS compatible, and can be incorporated into microlasers and serve as novel nanophotonic devices. Our investigations and results can be extended to multifunctional share-aperture metasurfaces in order to achieve multispectral mode shaping.<sup>36–38</sup>

## AUTHOR INFORMATION

### Corresponding Author

\*E-mail: nir.davidson@weizmann.ac.il.

### ORCID

Elhanan Maguid: 0000-0001-6972-1816

Erez Hasman: 0000-0002-3419-8815

### Author Contributions

<sup>§</sup>These authors contributed equally to this work.

### Notes

The authors declare no competing financial interest.

## ACKNOWLEDGMENTS

This research was supported by the Israel Ministry of Science, Technology and Space, the Israel Science Foundation (ISF). The fabrications of the metasurfaces were performed at the Micro-Nano Fabrication & Printing Unit (MNF&PU), Technion.

## REFERENCES

- (1) Oron, R.; Blit, S.; Davidson, N.; Friesem, A. a.; Bomzon, Z.; Hasman, E. The Formation of Laser Beams with Pure Azimuthal or Radial Polarization. *Appl. Phys. Lett.* **2000**, *77* (21), 3322.
- (2) Nixon, M.; Katz, O.; Small, E.; Bromberg, Y.; Friesem, A. A.; Silberberg, Y.; Davidson, N. Real-Time Wavefront Shaping through Scattering Media by All-Optical Feedback. *Nat. Photonics* **2013**, *7* (10), 919–924.
- (3) Ye, Y.; Wong, Z. J.; Lu, X.; Ni, X.; Zhu, H.; Chen, X.; Wang, Y.; Zhang, X. Monolayer Excitonic Laser. *Nat. Photonics* **2015**, *9* (11), 733–737.
- (4) Naidoo, D.; Roux, F. S.; Dudley, A.; Litvin, I.; Piccirillo, B.; Marrucci, L.; Forbes, A. Controlled Generation of Higher-Order Poincaré Sphere Beams from a Laser. *Nat. Photonics* **2016**, *10* (5), 327–332.
- (5) Miao, P.; Zhang, Z.; Sun, J.; Walasik, W.; Longhi, S.; Litchinitser, N. M.; Feng, L. Orbital Angular Momentum Microlaser. *Science* **2016**, *353* (6298), 464–467.
- (6) Wong, Z. J.; Xu, Y.-L.; Kim, J.; O'Brien, K.; Wang, Y.; Feng, L.; Zhang, X. Lasing and Anti-Lasing in a Single Cavity. *Nat. Photonics* **2016**, *10* (12), 796–801.

(7) Oron, R.; Davidson, N.; Friesem, A. A.; Hasman, E. Transverse mode shaping and selection in laser resonators. *Prog. Opt.* **2001**, *42* (6), 325–386.

(8) Zeitner, U. D.; Wyrowski, F.; Zellmer, H. External Design Freedom for Optimization of Resonator Originated Beam Shaping. *IEEE J. Quantum Electron.* **2000**, *36* (10), 1105–1109.

(9) Wynne, J. J. Generation of the Rotationally Symmetric TE<sub>01</sub> and TM<sub>01</sub> Modes from a Wavelength-Tunable Laser. *IEEE J. Quantum Electron.* **1974**, *QE-10* (2), 125–127.

(10) Shimshi, L.; Ishaaya, A. A.; Ekhouse, V.; Davidson, N.; Friesem, A. A. Passive Intra-Cavity Phase Locking of Laser Channels. *Opt. Commun.* **2006**, *263* (1), 60–64.

(11) Ishaaya, A. A.; Davidson, N.; Friesem, A. A. Passive Laser Beam Combining With Intracavity Interferometric Combiners. *IEEE J. Sel. Top. Quantum Electron.* **2009**, *15* (2), 301–311.

(12) Nixon, M.; Ronen, E.; Friesem, A. A.; Davidson, N. Observing Geometric Frustration with Thousands of Coupled Lasers. *Phys. Rev. Lett.* **2013**, *110*, 184102.

(13) Chriki, R.; Nixon, M.; Pal, V.; Tradonsky, C.; Barach, G.; Friesem, A. A.; Davidson, N. Manipulating the Spatial Coherence of a Laser Source. *Opt. Express* **2015**, *23* (10), 12989–12997.

(14) Knitter, S.; Liu, C.; Redding, B.; Khokha, M. K.; Choma, M. A.; Cao, H. Coherence Switching of a Degenerate VECSEL for Multimodality Imaging. *Optica* **2016**, *3* (4), 403.

(15) Biener, G.; Niv, A.; Kleiner, V.; Hasman, E. Formation of Helical Beams by Use of Pancharatnam–Berry Phase Optical Elements. *Opt. Lett.* **2002**, *27* (21), 1875.

(16) Bliokh, K. Y.; Niv, A.; Kleiner, V.; Hasman, E. Geometrodynamics of Spinning Light. *Nat. Photonics* **2008**, *2* (12), 748–753.

(17) Gorodetski, Y.; Niv, A.; Kleiner, V.; Hasman, E. Observation of the Spin-Based Plasmonic Effect in Nanoscale Structures. *Phys. Rev. Lett.* **2008**, *101*, 043903.

(18) Bliokh, K. Y.; Smirnova, D.; Nori, F. Quantum Spin Hall Effect of Light. *Science* **2015**, *348* (6242), 1448–1451.

(19) Bomzon, Z.; Kleiner, V.; Hasman, E. Pancharatnam–Berry Phase in Space-Variant Polarization-State Manipulations with Subwavelength Gratings. *Opt. Lett.* **2001**, *26* (18), 1424–1426.

(20) Bomzon, Z.; Biener, G.; Kleiner, V.; Hasman, E. Space-Variant Pancharatnam–Berry Phase Optical Elements with Computer-Generated Subwavelength Gratings. *Opt. Lett.* **2002**, *27* (13), 1141.

(21) Yu, N.; Genevet, P.; Kats, M. A.; Aieta, F.; Tietienne, J.-P.; Capasso, F.; Gaburro, Z. Light Propagation with Phase Discontinuities Reflection and Refraction. *Science* **2011**, *334* (October), 333–337.

(22) Ni, X.; Emani, N. K.; Kildishev, A. V.; Boltasseva, A.; Shalaev, V. M. Broadband Light Bending with Plasmonic Nanoantennas. *Science* **2012**, *335* (6067), 427.

(23) Pors, A.; Albrechtsen, O.; Radko, I. P.; Bozhevolnyi, S. I. Gap Plasmon-Based Metasurfaces for Total Control of Reflected Light. *Sci. Rep.* **2013**, *3*, 2155.

(24) Sun, J.; Wang, X.; Xu, T.; Kudyshev, Z. A.; Cartwright, A. N.; Litchinitser, N. M. Spinning Light on the Nanoscale. *Nano Lett.* **2014**, *14* (5), 2726–2729.

(25) Lin, D.; Fan, P.; Hasman, E.; Brongersma, M. L. Dielectric Gradient Metasurface Optical Elements. *Science* **2014**, *345* (6194), 298–302.

(26) Arbabi, A.; Horie, Y.; Bagheri, M.; Faraon, A. Dielectric Metasurfaces for Complete Control of Phase and Polarization with Subwavelength Spatial Resolution and High Transmission. *Nat. Nanotechnol.* **2015**, *10* (11), 937–943.

(27) Zheng, G.; Mühlender, H.; Kenney, M.; Li, G.; Zentgraf, T.; Zhang, S. Metasurface Holograms Reaching 80% Efficiency. *Nat. Nanotechnol.* **2015**, *10* (4), 308–312.

(28) Chong, K. E.; Staude, I.; James, A.; Dominguez, J.; Liu, S.; Campione, S.; Subramania, G. S.; Luk, T. S.; Decker, M.; Neshev, D. N.; Brener, I.; Kivshar, Y. S. Polarization-Independent Silicon Metadevices for Efficient Optical Wavefront Control. *Nano Lett.* **2015**, *15* (8), 5369–5374.

- (29) Wang, Q.; Rogers, E. T. F.; Gholipour, B.; Wang, C.-M.; Yuan, G.; Teng, J.; Zheludev, N. I. Optically Reconfigurable Metasurfaces and Photonic Devices Based on Phase Change Materials. *Nat. Photonics* **2016**, *10* (1), 60–65.
- (30) Pancharatnam, B. Y. S. Generalized Theory of Interference and Its Applications-I. *Proc. Ind. Acad. Sci.* **1956**, *44* (w 4), 247–262.
- (31) Berry, M. V. Quantal Phase Factors Accompanying Adiabatic Changes. *Proc. R. Soc. London, Ser. A* **1984**, *392*, 45–57.
- (32) Chriki, R.; Maguid, E.; Tradonsky, C.; Kleiner, V.; Friesem, A. A.; Davidson, N.; Hasman, E. Spin-controlled twisted laser beams: intra-cavity multi-tasking geometric phase metasurfaces. *Opt. Express* **2018**, *26* (2), 905–916.
- (33) Xu, L.; Chen, D.; Curwen, A. C.; Memarian, M.; Reno, J. L.; Itoh, T.; Williams, S. B. Metasurface quantum-cascade laser with electrically switchable polarization. *Optica*. **2017**, *4* (4), 468.
- (34) Xu, L.; Chen, D.; Itoh, T.; Reno, J. L.; Williams, S. B. Focusing metasurface quantum-cascade laser with a near diffraction-limited beam. *Opt. Express* **2016**, *24* (21), 24117–24128.
- (35) Mansuripur, M.; Zakharian, A. R.; Wright, E. M. Spin and orbital angular momenta of light reflected from a cone. *Phys. Rev. A: At, Mol, Opt. Phys.* **2011**, *84* (3), 033813.
- (36) Maguid, E.; Yulevich, I.; Veksler, D.; Kleiner, V.; Brongersma, M. L.; Hasman, E. Photonic Spin-Controlled Multifunctional Shared-Aperture Antenna Array. *Science* **2016**, *352* (6290), 1202–1206.
- (37) Lin, D.; Holsteen, A. L.; Maguid, E.; Wetzstein, G.; Kik, P. G.; Hasman, E.; Brongersma, M. L. Photonic Multitasking Interleaved Si Nanoantenna Phased Array. *Nano Lett.* **2016**, *16* (12), 7671–7676.
- (38) Maguid, E.; Yulevich, I.; Yannai, M.; Kleiner, V.; L Brongersma, M.; Hasman, E. Multifunctional Interleaved Geometric-Phase Dielectric Metasurfaces. *Light: Sci. Appl.* **2017**, *6* (8), e17027.